

Enhanced Rashba spin-orbit splitting in Bi/Ag(111) and Pb/Ag(111) surface alloys from first principles

G. Bihlmayer,^{1,*} S. Blügel,¹ and E. V. Chulkov^{2,3}¹*Institut für Festkörperforschung, Forschungszentrum Jülich, D-52425 Jülich, Germany*²*Donostia International Physics Center, San Sebastián/Donostia, Basque Country 20018, Spain*³*Departamento de Física de Materiales and Centro Mixto CSIC-UPV/EHU, UPV/EHU, Apartado 1072, San Sebastián/Donostia, Basque Country 20080, Spain*

(Received 23 January 2007; revised manuscript received 7 March 2007; published 11 May 2007)

We present first-principles calculations of a $(\sqrt{3} \times \sqrt{3})R30^\circ$ Bi/Ag(111)-ordered surface alloy, which has recently been investigated experimentally using angle-resolved photoemission spectroscopy. The surface states in the L -projected bulk band gap show a Rashba-type spin-orbit splitting which is three times larger than what has been observed on a clean Bi(111) surface. This large enhancement can be explained by the strong distortion of the surface-state wave function which is caused by the substantial outward buckling of the Bi atom. Also, in a similar surface alloy, Pb/Ag(111), a strong Rashba-type splitting was found by our calculations. The comparison to the experimental data is more difficult due to the presence of a second, close-by surface state. We discuss the dependence of the two-dimensional band structure on the surface corrugation and compare to the experimental findings.

DOI: [10.1103/PhysRevB.75.195414](https://doi.org/10.1103/PhysRevB.75.195414)

PACS number(s): 73.20.At, 71.70.Ej, 71.15.Mb

I. INTRODUCTION

Surface states, which can be regarded to form a two-dimensional electron gas in the surface (x, y) plane, are frequently described in terms of the kinetic energy of electron with an effective mass m^* . Due to the relativistic effects, an electric field \mathbf{E} (e.g., the potential gradient normal to the surface) is seen by the moving electrons as a magnetic field that couples to the spin of the electron. This effect, known as the Rashba effect or Rashba spin-orbit coupling,¹ is described by the Bychkov-Rashba Hamiltonian,^{2,3}

$$H_R = \alpha_R(|\mathbf{E}|)\boldsymbol{\sigma} \cdot (\mathbf{k}_{\parallel} \times \hat{\mathbf{e}}_z), \quad (1)$$

where $\mathbf{k}_{\parallel} = (k_x, k_y, 0)$ characterizes the crystal momentum of a surface electron, $\boldsymbol{\sigma}$ are the Pauli matrices, and $\hat{\mathbf{e}}_z = (0, 0, 1)$. α_R is called the Rashba parameter. Thus, the spin degeneracy of the two-dimensional electron gas provided by the surface states is lifted and the energy dispersion has the form

$$E_{\text{RSO}} = \frac{\hbar^2}{2m^*} (k_{\parallel} \pm \Delta k)^2 - E_{\text{SO}}. \quad (2)$$

Here, E_{SO} is the energy associated with the k -independent, atomic spin-orbit coupling. Equation (2) describes two parabolas that are shifted $\pm \Delta k$ around the origin. In semiconductor heterostructures, the Rashba effect has gained considerable attention, e.g., as a concept to realize a spin transistor for spintronics applications.⁴

Surface states can show a Rashba-type spin-orbit splitting which is much larger than what is known from semiconductor heterostructures. In retrospect, the first observation of this kind of splitting was made ten years ago on the Au(111) surface⁵ using angle-resolved photoemission spectroscopy (ARPES). Since then, this effect was observed on several surfaces of heavy elements,^{6–18} most noticeably Bi(111),^{14–16} Bi(100),¹⁸ and Bi(110).¹³ On the Bi surfaces, the splitting is much larger than on Au(111) so that it was not *a priori* clear

which of the observed features were spin-split partners of the same state or two different surface states. Later, calculations based on density-functional theory (DFT) provided the necessary information.¹⁵ Recently, ARPES measurements of a $(\sqrt{3} \times \sqrt{3})R30^\circ$ Bi/Ag(111) surface alloy have shown an occupied surface state in the L -projected bulk band gap of Ag(111), which has a Rashba-type splitting three times larger than the Bi(111) surface state.¹⁹

There are some aspects which make this result quite surprising. First, spin-orbit splitting on the Ag(111) surface is small: in photoemission measurements, this splitting has not been detected.²⁰ Of the three atoms per surface unit cell in the topmost layer of the surface alloy only one is Bi, all others (including deeper layers) are Ag. Second, the most significant contributions to the spin-orbit splitting result from all regions with strong variation of the one-electron potential, namely, from small areas centered at surface and subsurface layer atom positions and from the surface charge-density variation in this region.^{21,22} These charge and/or potential gradients have to be perpendicular to the propagation directions of the surface electrons, i.e., in the direction of the surface normal. There is no reason to expect that these gradients are much larger in the Bi/Ag surface alloy than on the clean Bi(111) surface, which are both close packed in structure. Also, as we will show, the work functions of Bi(111) and the Bi/Ag(111) surface alloy are rather similar. Therefore, one can in total expect a smaller spin-orbit splitting on the $(\sqrt{3} \times \sqrt{3})R30^\circ$ Bi/Ag(111) surface compared to that on Bi surfaces.^{13,15,23} The aim of this work is to unravel the origin of this large enhancement of the spin splitting.

Very recently, ARPES measurements have also been performed on an ordered $(\sqrt{3} \times \sqrt{3})R30^\circ$ Pb/Ag(111) surface alloy. A similar surface state was observed but surprisingly the Rashba-type splitting seems to be significantly smaller compared to the Bi case.²⁴ This is rather unexpected, since the nuclear numbers of lead and bismuth are very similar (82 and 83, respectively). Although lead has a smaller atomic

spin-orbit splitting than bismuth, this effect is too small to explain the origin of the difference between these two surface alloys. Since the Pb/Ag(111) surface state is unoccupied at the $\bar{\Gamma}$ point, ARPES experiments cannot directly compare the band dispersions in the Bi and Pb cases. Our calculations show that, in fact, the Rashba-type spin-orbit splitting is similar in both cases, but other partially occupied surface states can complicate the interpretation of the spectra of the lead alloy.

II. METHOD

For the calculations we employed DFT in the generalized gradient approximation (GGA) of Perdew *et al.*²⁵ We use the full-potential linearized augmented plane-wave method^{26,27} as realized in the FLEUR code.²⁸ We set the muffin-tin radii to $R_{MT}=2.4$ a.u. (Ag) and 2.5 a.u. (Pb, Bi). The plane wave cutoff for the basis functions was $K_{max}=3.8$ a.u.⁻¹ and the irreducible wedge of the Brillouin zone was sampled with 19 \mathbf{k} points for the scalar relativistic calculations. Spin-orbit coupling (SOC) was included in the self-consistent calculations, as described in Ref. 29.

A ten-layer film embedded in vacuum was used to simulate the surface. We assumed a $(\sqrt{3} \times \sqrt{3})R30^\circ$ unit cell with two Ag and one Pb or Bi atom on the surface. We optimized the positions of the atoms in the outermost four layers and observed a considerable outward relaxation of the Bi and Pb atoms. The bucklings of the surface layer were 0.85 and 0.97 Å, for Bi and Pb, respectively. The structural optimization was performed both without and with SOC included, but spin-orbit coupling affects only the position of the Bi and Pb atoms by about 0.05 Å, which is small compared to the actual relaxations. In the surface band structures, we considered states which have more than 12% charge in the surface Bi and 6% charge in the surface Ag atoms as surface states.

III. RESULTS

A. Bi/Ag(111)

Recent experiments have shown that a commensurate $(\sqrt{3} \times \sqrt{3})R30^\circ$ Bi/Ag surface alloy can be grown on a Ag(111) substrate.¹⁹ Topographic maps recorded with scanning tunneling microscopy show a long-range-ordered substitutional alloy with a Bi content of 33% and ARPES measurements revealed a Bi-related surface state in the L -projected bulk-band gap of Ag(111). In the $(\sqrt{3} \times \sqrt{3})R30^\circ$ unit cell, this projected band gap is actually a superposition of two projected band gaps, one around $\bar{\Gamma}$, the other around \bar{K} , of the Ag(111) surface.³⁰ (A schematic illustration of the unfolded and backfolded Brillouin zones can be found in Ref. 24.) This backfolding leaves the width of the band gap at the Fermi level unchanged (± 0.25 Å⁻¹ around the $\bar{\Gamma}$ point), but confines it at higher energies to about 2.5 eV with respect to the Fermi level at $\bar{\Gamma}$. As can be seen in Fig. 1, four surface states can be found in this region. Considering only the band structure generated without inclusion of SOC (left of Fig. 1), we can identify at $\bar{\Gamma}$ at the Fermi

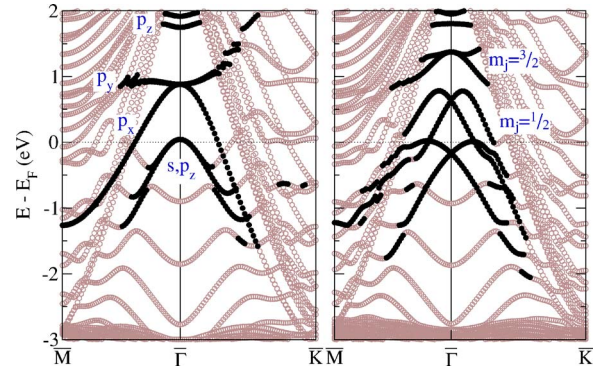


FIG. 1. (Color online) Band structure of $(\sqrt{3} \times \sqrt{3})R30^\circ$ Bi/Ag(111) without (left) and with spin-orbit coupling included (right). States which are localized mainly in the surface layer are marked with filled circles. The labels in the left figure refer to the orbital character [with increasing energy: (s, p_z) , p_x , p_y , p_z] of the surface states. The labels in the right figure indicate the effect of spin-orbit coupling on the p_x and p_y states. The distance between $\bar{\Gamma}$ and \bar{M} corresponds to 0.72 Å⁻¹.

level a downward dispersing Bi (s, p_z) -like surface state and at around 1 eV above E_F the degenerate p_x - and p_y -type surface states. In $\bar{\Gamma}\bar{M}$ direction, the orbital that points in the direction of the nearest-neighbor Bi atom (p_x) remains localized in the surface layer and disperses down to -1.2 eV, while the other p orbital shows little dispersion and hybridizes with the Ag states at the edge of the projected band gap. In the $\bar{\Gamma}\bar{K}$ direction this (p_y) orbital shows an upward dispersion, while the p_x state disperses to lower energies. At about 1.8 eV, a p_z -like surface state can be seen. At this energy, the surface-state wave function penetrates so deep into the Ag bulk that the energy levels split due to the interaction between the upper and the lower surface of the symmetric ten-layer film that is used to simulate the surface of the semiinfinite crystal.

In the ARPES experiment, two downward dispersing parabolic states are seen, which are shifted by ± 0.16 Å⁻¹ away from the $\bar{\Gamma}$ point. This is the typical signature of a Rashba-type splitting of the surface state, which cannot be reproduced in a calculation without spin-orbit coupling. Therefore, we repeat the surface band-structure calculation with the inclusion of SOC (right panel of Fig. 1). The (s, p_z) state can be seen to split symmetrically around the zone center by ± 0.13 Å⁻¹, in good agreement with experimental data. The calculated energy position of this state at $\bar{\Gamma}$ is slightly higher (-0.2 eV) than the measured one (-0.3 eV). We notice that SOC removes the degeneracy of the p_x - and p_y -type states at the $\bar{\Gamma}$ point and forms orbital moment carrying $p_{(x,y)}$ states that can be classified as $m_j = \frac{1}{2}$ (at 0.6 eV) and $m_j = \frac{3}{2}$ (at 1.3 eV).

At about the $k_{||}$ position of the maximum of the (s, p_z) surface state (i.e., ± 0.13 Å⁻¹), a band crossing with the $m_j = \frac{1}{2}$ surface state can be seen. Also, in the experimental data, an indication of this state could be present, although it is difficult to see since its intensity is weaker and it is located at the edge of the observation window in Ref. 19. These two

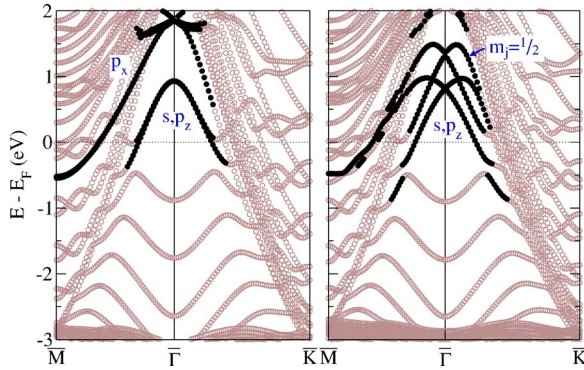


FIG. 2. (Color online) Band structure of $(\sqrt{3} \times \sqrt{3})R30^\circ$ Pb/Ag(111) without (left) and with spin-orbit coupling included (right). States which are localized mainly in the surface layer are marked with filled circles.

surface states can be seen to hybridize more strongly when the outward relaxation of the Bi atom is artificially reduced. In this case, a gap opens at the band crossing and the Rashba splitting of the (s, p_z) surface state seems to decrease, as will be discussed below. From Fig. 1, we can also see that the size of the splitting of the two surface states, (s, p_z) and $m_j = \frac{1}{2}$, is considerably different. This is not unexpected, since spin-orbit coupling affects $p_{(x,y)}$ states differently from p_z -derived states.³¹ This is even more evident in the case of the $m_j = \frac{3}{2}$ state, which shows a spin-orbit-induced splitting which is proportional to k^3 (best seen in $\bar{\Gamma}\bar{K}$ direction), while the splitting of the other surface states is dominated by a term linear in k .

At small binding energies, e.g., 0.18 eV, the (s, p_z) and $m_j = \frac{1}{2}$ surface states form four distinctive features in the \mathbf{k}_\parallel plane, two circular cuts with radii of 0.04 and 0.17 \AA^{-1} and two hexagonal cuts with side lengths of about 0.25 and 0.32 \AA^{-1} . It might be interesting to note that these hexagons are rotated by 30° with respect to the surface Brillouin zone and also with respect to the projected bulk band gap of the Ag states in this energy region.

B. Pb/Ag(111)

Let us now turn to the second system, Pb/Ag(111) ($\sqrt{3} \times \sqrt{3})R30^\circ$, where a spin-orbit split surface state has also been observed experimentally.²⁴ In this surface alloy, a surface band structure similar to the Bi alloy is obtained, but—since lead is to the left of bismuth in the Periodic Table and has one p electron less than in Bi—the (s, p_z) surface state is unoccupied at the $\bar{\Gamma}$ point (see Fig. 2). The band structure of the Pb/Ag(111) surface alloy has been calculated before, but without the inclusion of spin-orbit coupling.²⁴ We, therefore, just notice the similarity of the observed states with the Bi case, and directly discuss the band structure calculated with SOC (right of Fig. 2). For the (s, p_z) surface state, we find the maxima of the dispersion curves at $\pm \Delta k = \pm 0.11 \text{\AA}^{-1}$. This is slightly smaller than in the Bi alloy, but still much larger than in the clean Bi(111) surface. We also notice that the separation between the (s, p_z) and $m_j = \frac{1}{2}$ states is now smaller than

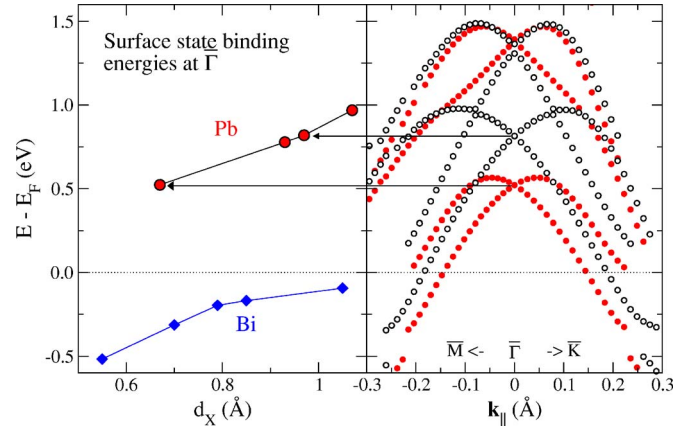


FIG. 3. (Color online) Left: Variation of the energy position at $\bar{\Gamma}$ of the (s, p_z) -type surface state (E) as a function of relaxation of the Bi/Pb atom normal to the surface. d_X is the distance from the atom X to the plane of the topmost Ag atoms. Right: Dispersion of Pb/Ag(111) surface states for two different relaxations d_{Pb} : 0.67 \AA (filled circles) and 0.97 \AA (open circles).

in the Bi/Ag(111) surface alloy. Therefore, these two states cross at 0.08\AA^{-1} and get as close as 0.07\AA^{-1} at larger \mathbf{k} vectors. Again, this crossing is sensitive to the relaxation of the Pb atom and a smaller Pb-Ag distance leads to an opening of a gap between these two branches (see right of Fig. 3).

Experimentally, near the $\bar{\Gamma}$ point, two surface-state branches have been observed, which seem to originate from a Rashba spin-orbit split state which disperses downward from 0.6 eV at $\bar{\Gamma}$ and crosses the Fermi level at 0.13 and 0.18 \AA^{-1} in $\bar{\Gamma}\bar{K}$ direction.²⁴ Compared to our calculation, the Fermi level E_F seems to be shifted by about 0.3 eV. The positions of surface states in ARPES and DFT calculations normally differ by not more than 50–100 meV for these type of systems, so the discrepancy is unusually large in the case of Pb/Ag(111). From Fig. 3, it can be seen that for a relaxation of 0.67 \AA (i.e., 0.3 \AA smaller than what would be expected from the calculation) not only the binding energy of the surface state at $\bar{\Gamma}$ has shifted by 300 meV but also the so-called Rashba energy (the energy difference between the extremum of the dispersion curves and their crossing point) is a factor of 3 smaller. This would indicate a Rashba splitting that is a factor of 3 smaller, as it is observed experimentally.

Experimentally, also a Pb-derived surface state at the \bar{M} point was observed: originating at about -1.1 eV, this state disperses upward in $\bar{M}\bar{\Gamma}$ direction and downward in $\bar{M}\bar{K}$. This state can be identified as a mixture of the (s, p_z) and $m_j = \frac{1}{2}$ states that are shifted further away from the $\bar{\Gamma}$ point. They can be observed in the calculation at about -0.8 eV at \bar{M} , i.e., again 0.3 eV higher than in the experiment.

IV. DISCUSSION

Let us now go back to the question stated in the Introduction: Why is the Rashba-type splitting in the Bi/Ag alloy so much larger than in Bi(111)? As we have already noted

above, surface states of different characters show different splittings, not only quantitatively but also qualitatively (linear vs. cubic in k). The Bi(111) surface state is not localized solely in the surface layer but rather forms a bond between surface and subsurface atoms. It is of $p_{(x,y)}$ character in the subsurface layer, while in the surface more p_z character can be found, but not exclusively. In a (hypothetical) flat Bi/Ag(111) surface alloy, the occupied surface state is of (s, p_z) type with an $s:p_z$ ratio of 4:1. The Rashba-type splitting in this case is about 0.05 \AA^{-1} , thus in the range of clean Bi(111). A small outward relaxation of the Bi atom (0.1 \AA) changes this ratio to 2:1, thus increasing the splitting to about 0.07 \AA^{-1} . Further relaxation (0.87 \AA) adds also some $p_{(x,y)}$ character at the expense of s character to the surface state and increases the splitting even more to $\Delta k=0.13 \text{ \AA}^{-1}$. It is not unusual that a change in the character of the surface state is reflected in a strong change of the value of Δk : for Bi(110) even $\Delta k=0.17 \text{ \AA}^{-1}$ was found.¹⁵

From our calculations, we found that both the Bi and the Pb surface alloy (s, p_z) surface states have very strong Rashba splittings of $\Delta k=0.13$ and $\Delta k=0.11 \text{ \AA}^{-1}$, respectively. Experimentally, for the bismuth alloy $\Delta k=0.13\text{--}0.16 \text{ \AA}^{-1}$ was found, depending on the temperature and experimental method used to determine the splittings.¹⁹ For the lead alloy, however, a fit to the measured spectra indicated $\Delta k=0.03 \text{ \AA}^{-1}$, i.e., the two branches visible at the Fermi level are separated by 0.06 \AA^{-1} . As compared to our calculation, the position of the surface state at $\bar{\Gamma}$ seems to be 0.3 eV too high. At an energy of 0.3 eV above E_F , we also observe two dispersion curves, related to the (s, p_z) and $m_j = \frac{1}{2}$ states, separated by 0.07 \AA^{-1} . This could be interpreted as originating from a single, Rashba-split state with $\Delta k=0.035 \text{ \AA}^{-1}$. As noted above, depending on the relaxation, the (s, p_z) and $m_j = \frac{1}{2}$ states can hybridize more or less strongly, so that it is not strictly possible to say whether the two observed branches originate from two surface states with strong Rashba splitting or from a single state with a smaller splitting. Since the spectral intensities of the two states are quite different in the experiment (Ref. 24), one might be inclined in favor of the former interpretation.

There are, however, also considerable uncertainties as far as the comparison of theory and experiment is concerned. For example, the position and the Rashba splitting of the surface state depend sensitively on the relaxation of the Pb or Bi atom in the alloy. As can be seen in the left of Fig. 3, with decreasing relaxation the energetical position of the state decreases continuously. Experimentally, the structure of the Pb/Ag(111) $(\sqrt{3} \times \sqrt{3})R30^\circ$ surface alloy has been investigated by surface x-ray diffraction and scanning tunneling microscopy.³² While the latter method indicated a corrugation of $d_{pb}=0.8 \text{ \AA}$, the former experiment yields a much smaller value of 0.45 \AA . Moreover, the two Ag atoms in the surface layer were found to have a slightly different inward relaxation, a finding that cannot be supported by our calculations. This reference also includes calculations based on a simplified tight-binding scheme, where a value of $d_{pb}=0.68 \text{ \AA}$ was obtained. In Ref. 24, also a structural optimization was performed, but no results are given. Our DFT calculation using GGA leads to a large relaxation of 0.97 \AA ,

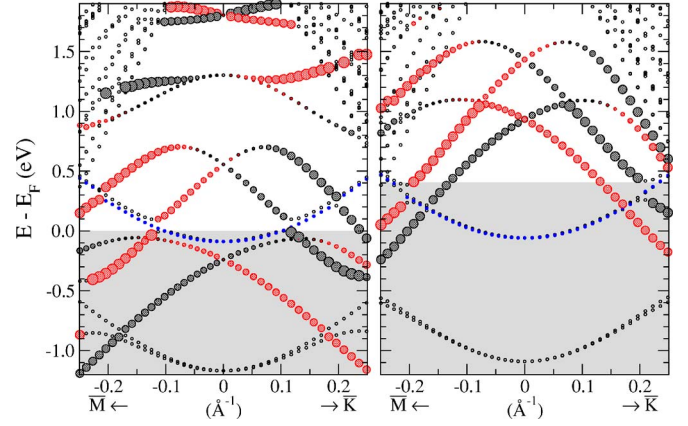


FIG. 4. (Color online) Band structure of an asymmetric film with a $(\sqrt{3} \times \sqrt{3})R30^\circ$ Bi/Ag(111) (left) and Pb/Ag(111) (right) surface alloy on one side and a clean Ag(111) surface on the opposite side. The Ag(111) surface state is marked in blue, and the Bi and Pb states are marked with red and black circles. The size of the circles indicates the degree of spin polarization of the states, and the color distinguishes the different spin directions; the spin-quantization axis was chosen perpendicular to the surface normal and to the propagation direction (\mathbf{k}_\parallel).

and therefore, according to Fig. 3, also to a large (negative) binding energy of the surface state. Why the calculated data for Bi/Ag(111) fit the experiment nicely, while in the case of Pb/Ag(111) some differences between theory and experiment remain unresolved, is not clear at the moment.

We checked the reliability of our results with respect to the different computational parameters, e.g., the determination of the Fermi level or the thickness of the film. To exclude an eventual interaction between the two surface states of a symmetric film setup, we calculated the band structure of an asymmetric ten-layer film with a $(\sqrt{3} \times \sqrt{3})R30^\circ$ Bi/Ag(111) and Pb/Ag(111) surface alloy on one side and a clean Ag(111) surface on the opposite side. As can be seen in Fig. 4, the position of the surface states is not significantly changed; we also find the Ag surface state of the clean Ag(111) surface at a position which is in good agreement with the experimental value. We also verified that this picture does not depend on the employed exchange-correlation potential, i.e., GGA and the local density approximation give qualitatively similar results. In summary, we find that the experimental data are nicely reproduced for the bismuth alloy, while for the lead alloy the experimental observation seems to refer to a different Fermi level, indicated by the shaded region in Fig. 4.

Finally, we want to discuss the spin polarization of the surface states observed in Fig. 4. It might be interesting to note that around the $\bar{\Gamma}$ point, the (s, p_z) and p_z surface states (at 1.8 eV in the Bi alloy) show the usual, Rashba-type spin splitting, i.e., the two parabolas shifted by Δk from the center of the Brillouin zone are populated by electrons of opposite spins. The situation gets a bit more involved at larger wave vectors [e.g., at $k=0.15 \text{ \AA}^{-1}$ around the Fermi level in the Bi/Ag(111) alloy], where hybridization occurs and the spin polarization decreases and finally even changes its sign. Even more involved is the situation for the $p_{(x,y)}$ states,

which are coupled by (atomiclike) spin-orbit coupling to $m_j = \pm \frac{1}{2}$ and $m_j = \pm \frac{3}{2}$ states. This is clearly seen at the $\bar{\Gamma}$ point, where these states are split by 0.8 eV. (In semiconductors, a similar lifting of degeneracy in a fourfold degenerate band is termed light-hole heavy-hole splitting, see, e.g., Ref. 31.) The (lower) $m_j = \pm \frac{1}{2}$ state shows at small k_{\parallel} a Rashba-type (linear k) splitting, while the higher lying state is split by terms of higher order in k .³¹ At larger values of k_{\parallel} , both branches of the $m_j = \pm \frac{1}{2}$ state are populated by electrons of the same spin. A similar situation is found for the $m_j = \pm \frac{3}{2}$ state, but at $k_{\parallel} = 0.15 \text{ \AA}^{-1}$, the spin polarization of the lower branch changes sign, i.e., at the same wave vector where the change in polarization was observed in the (s, p_z) state. This change of the spin orientation is a phenomenon that can appear in $j = \frac{3}{2}$ electron systems³³ and will not occur in Rashba-split (s, p_z) bands. That it can nevertheless be observed near the crossing point of the $m_j = \frac{1}{2}$ and (s, p_z) band indicates a partial hybridization between these two bands. This hybridization creates the impression that the change of spin orientation occurs in the (s, p_z) band, not in the $m_j = \frac{1}{2}$ where it would be expected. In summary, we observe that the situation is far more complex than in similar systems where only a single p_z surface state is present [e.g., in Au(111)].

V. SUMMARY

We have investigated the surface electronic structure of the ordered surface alloys of Bi/Ag(111) and Pb/Ag(111).

These alloys provide model systems to study the Rashba-type spin-orbit splitting of surface states of different characters in the same environment. Comparison with recent experimental data of the occupied part of the band structure shows good agreement in the case of Bi/Ag(111), while for Pb/Ag(111) some differences remain. The unoccupied part of the spectrum was also studied using scanning tunneling spectroscopy,³⁴ and also here the Bi/Ag(111) spectrum seems to be nicely reproduced, while for the lead alloy the surface-state position is too high in the calculations as compared to the experiment. Since the surface-state position and the corrugation of the surface are intimately connected, a smaller corrugation could account for the experimental data. More experimental work on the surface structure is, therefore, desirable. Our calculations also suggest that an experimental investigation of the spin polarization of these surface states could be quite interesting, since the polarization can be quite different for different branches and can even change its sign within a single branch.

ACKNOWLEDGMENTS

We acknowledge valuable discussions with C. R. Ast, A. Bringer, and K. Kern, and thank C. R. Ast for making some of his experimental data available to us before publication.

*Electronic address: g.bihlmayer@fz-juelich.de

¹E. I. Rashba, Sov. Phys. Solid State **2**, 1109 (1960).

²Y. A. Bychkov and E. I. Rashba, J. Phys. C **17**, 6039 (1984).

³Y. A. Bychkov and E. I. Rashba, JETP Lett. **39**, 78 (1984).

⁴S. Datta and B. Das, Appl. Phys. Lett. **56**, 665 (1990).

⁵S. LaShell, B. A. McDougall, and E. Jensen, Phys. Rev. Lett. **77**, 3419 (1996).

⁶E. Rotenberg, J. W. Chung, and S. D. Kevan, Phys. Rev. Lett. **82**, 4066 (1999).

⁷M. Hochstrasser, J. G. Tobin, E. Rotenberg, and S. D. Kevan, Phys. Rev. Lett. **89**, 216802 (2002).

⁸O. Krupin, G. Bihlmayer, K. Starke, S. Gorovikov, J. E. Prieto, K. Döbrich, S. Blügel, and G. Kaindl, Phys. Rev. B **71**, 201403(R) (2005).

⁹F. Schiller, R. Keyling, E. V. Chulkov, and J. E. Ortega, Phys. Rev. Lett. **95**, 126402 (2005).

¹⁰F. Reinert, G. Nicolay, S. Schmidt, D. Ehm, and S. Hüfner, Phys. Rev. B **63**, 115415 (2001).

¹¹J. Henk, M. Hoesch, J. Osterwalder, A. Ernst, and P. Bruno, J. Phys.: Condens. Matter **16**, 7581 (2004).

¹²M. Hoesch, M. Muntwiler, V. N. Petrov, M. Hengsberger, L. Patthey, M. Shi, M. Falub, T. Greber, and J. Osterwalder, Phys. Rev. B **69**, 241401(R) (2004).

¹³S. Agergaard, C. Søndergaard, H. Li, M. B. Nielsen, S. V. Hoffmann, Z. Li, and Ph. Hofmann, New J. Phys. **3**, 15 (2001).

¹⁴C. R. Ast and H. Höchst, Phys. Rev. Lett. **87**, 177602 (2001).

¹⁵Yu. M. Koroteev, G. Bihlmayer, J. E. Gayone, E. V. Chulkov, S. Blügel, P. M. Echenique, and Ph. Hofmann, Phys. Rev. Lett. **93**,

046403 (2004).

¹⁶T. Hirahara, T. Nagao, I. Matsuda, G. Bihlmayer, E. V. Chulkov, Yu. M. Koroteev, P. M. Echenique, M. Saito, and S. Hasegawa, Phys. Rev. Lett. **97**, 146803 (2006).

¹⁷K. Sugawara, T. Sato, S. Souma, T. Takahashi, M. Arai, and T. Sasaki, Phys. Rev. Lett. **96**, 046411 (2006).

¹⁸Ph. Hofmann, J. E. Gayone, G. Bihlmayer, Yu. M. Koroteev, and E. V. Chulkov, Phys. Rev. B **71**, 195413 (2005).

¹⁹C. R. Ast, D. Pacilé, M. Falub, L. Moreschini, M. Papagno, G. Wittich, P. Wahl, R. Vogelgesang, M. Grioni, and K. Kern, arXiv:cond-mat/0509509 (unpublished).

²⁰F. Reinert, J. Phys.: Condens. Matter **15**, S693 (2003).

²¹A. Mugarza, A. Mascaraque, V. Repain, S. Rousset, K. N. Altmann, F. J. Himpsel, Yu. M. Koroteev, E. V. Chulkov, F. J. García de Abajo, and J. E. Ortega, Phys. Rev. B **66**, 245419 (2002).

²²G. Bihlmayer, Yu. M. Koroteev, P. M. Echenique, E. V. Chulkov, and S. Blügel, Surf. Sci. **600**, 3888 (2006).

²³Ph. Hofmann, Prog. Surf. Sci. **81**, 191 (2006).

²⁴D. Pacilé, C. R. Ast, M. Papagno, C. DaSilva, L. Moreschini, M. Falub, A. P. Seitsonen, and M. Grioni, Phys. Rev. B **73**, 245429 (2006).

²⁵J. P. Perdew, K. Burke, and M. Ernzerhof, Phys. Rev. Lett. **77**, 3865 (1996).

²⁶E. Wimmer, H. Krakauer, M. Weinert, and A. J. Freeman, Phys. Rev. B **24**, 864 (1981).

²⁷M. Weinert, E. Wimmer, and A. J. Freeman, Phys. Rev. B **26**, 4571 (1982).

- ²⁸<http://www.flapw.de>
- ²⁹C. Li, A. J. Freeman, H. J. F. Jansen, and C. L. Fu, Phys. Rev. B **42**, 5433 (1990).
- ³⁰K.-M. Ho, C.-L. Fu, S. H. Liu, D. M. Kolb, and G. Piazza, J. Electroanal. Chem. Interfacial Electrochem. **150**, 235 (1983).
- ³¹R. Winkler, *Spin-Orbit Coupling Effects in Two-Dimensional Electron and Hole Systems*, Springer Tracts in Modern Physics Vol. 191 (Springer, Berlin, 2003).
- ³²J. Dalmas, H. Oughaddou, C. Léandri, J.-M. Gay, G. Le Gay, G. Tréglia, B. Aufray, O. Bunk, and R. L. Johnson, Phys. Rev. B **72**, 155424 (2005).
- ³³R. Winkler, Phys. Rev. B **71**, 113307 (2005).
- ³⁴C. R. Ast, G. Wittich, P. Wahl, R. Vogelgesang, D. Pacilé, M. C. Falub, L. Moreschini, M. Papagno, M. Grioni, and K. Kern, Phys. Rev. B **75**, 201401(R) (2007).